

Very high-energy γ -ray observations of the Crab nebula with the GRAAL experiment

F. Arqueros¹, J. Ballestrín², D. M. Borque¹, M. Díaz⁵, R. Enríquez¹, H.-J. Gebauer⁵, and R. Plaga⁵

¹Facultad de Ciencias Físicas, Universidad Complutense, E-28040 Madrid, Spain

²CIEMAT-Departamento Energías Renovables, , Plataforma Solar de Almería, E-04080 Almería, Spain

⁵Max-Planck-Institut für Physik, 80805 München, Germany

Abstract. The “Gamma Ray Astronomy at ALmería” (GRAAL) experiment uses 63 heliostat-mirrors with a total mirror area of $\approx 2500 \text{ m}^2$ from the CESA-1 field to collect Cherenkov light from airshowers. The detector is located in a central solar tower and detects photon-induced showers with an energy threshold of $250 \pm 110 \text{ GeV}$ and an asymptotic effective detection area of about 15000 m^2 .

Data sets taken in the period September 1999 - September 2000 in the direction of the Crab pulsar were analysed for high energy γ -ray emission. In an analysis searching for an excess of events from the direction of the source evidence for γ -ray flux from the Crab pulsar with an integral flux of 2.2 ± 0.4 (stat) $^{+1.9}_{-1.5}$ (syst) $\times 10^{-9} \text{ cm}^{-2} \text{ s}^{-1}$ above threshold and a significance of 4.5σ in a total (usable) observing time of 7 hours and 10 minutes on source was found. However, no evidence for an excess in the total counting rate was found. No evidence for emission from the other sources was seen.

1 Introduction

Measuring atmospheric Cherenkov radiation is presently the most effective way to detect cosmic γ -rays with primary energies between about 100 GeV and 1 TeV (F.Krennrich (2001)). In order to reach low energy thresholds with techniques based on Cherenkov light, large mirror collection areas are needed. GRAAL is an experiment that employs the large mirror area of an existing tower solar-power plant for this purpose. This contribution describes the experimental results of one season of observation of the Crab pulsar, another one (F.Arqueros et al. (2001b)) describes the results of Monte-Carlo studies and what can be learned from them. A more detailed account of our results has been submitted recently (F.Arqueros et al. (2001)).

2 The GRAAL detector

CESA-1 is a heliostat field comprising of 225 steerable mirrors to the north of a central tower located within the

“Plataforma Solar de Almería”(PSA), a solar thermal-energy research centre located in the desert of Tabernas ($37^\circ.095 \text{ N}$, $2^\circ.360 \text{ W}$) at a height a.s.l. of 505 m. The 63 heliostats used for GRAAL have a mirror area of 39.7 m^2 each and have a roughly spherical shape.

The heliostats focus the Cherenkov light of airshowers from the direction of potential gamma-ray sources to software adjustable “aiming points” in the central tower (see fig.1). Cherenkov light from four groups of heliostats (with 13,14,18,18 members, respectively) is directed onto four single non-imaging “cone concentrators” (truncated Winston cones with an opening angle of 10°) each containing a single large-area PMT. They are housed in a special enclosure that is fastened to the outside of the central tower at a height of 70 m. The incoming light from an air shower consists of a train of pulses from the different heliostats, usually fully separated by pathlength differences. The arrival time and amplitude of each heliostat can thus be determined with a flash-ADC in a sequential mode.

Compared to the three other heliostat field experiments (“CELESTE”(M. de Naurois et al. (2000)), “STACEE”(M.C. Chantell et al. (1998)) and “Solar 2” (A.Zweerink et al. (1999))) which focus the light of single heliostats onto related single PMT’s, the night-sky background (NSB) per channel is about a factor 10 higher in GRAAL (8-10 p.e./ns). This leads to a higher energy threshold. The advantage of the non-imaging approach is its greater simplicity leading to cost savings by about a factor 5-10 in hardware costs. The presence of only four data-acquisition channels makes automatization and remote control more feasible, leading to comparable savings in operation costs. In the non-imaging approach it is impossible to avoid a temporal overlap of the signal from certain heliostats depending on the pointing direction. This reduces the number of times/amplitudes usable in the reconstruction by about 20 %. On the positive side, calibration is easier when signals from several heliostats are measured in the same PMT.

We register all four pulse trains in only one Digital Oscilloscope with a bandwidth of 1 GHz and a time bin of 500 psec.

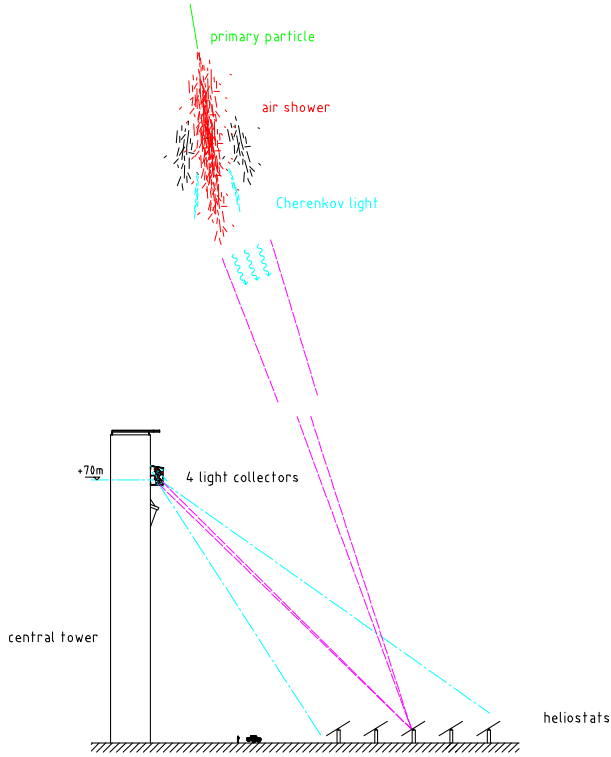


Fig. 1. Scheme of the experiment seen from the side, north is to the right. The Cherenkov light of a schematic airshower (not to scale with respect to the field) is concentrated by the heliostats of the CESA-1 field to a focus at the central tower. A dedicated platform mounted at the outside of the tower at the 70 m level houses four Winston cones which receive light from 13 - 18 heliostats in the field. The data-acquisition electronics is located inside the tower.

This ensures that the FWHM of individual pulses of about 3.6 nsec is negligibly increased by electronics effects. The time and amplitude calibration of our setup is performed using blue LEDs with a calibrator module that is fastened at the window of the Winston cones.

All operations (like opening of the door, high-voltage control etc.) at the central receiver and the tracking of the heliostat field are under remote control via the internet. Under conditions that indicate some malfunction, a physicist on shift is phoned by the PC and can check all parameters and images of web cameras, remotely. For the operation of the heliostat field and emergencies only the regular night-operator of the PSA is on-site in all observation nights. GRAAL is taking data continuously since August 1999 (since March 2000 in the final hardware configuration). Here we present data for the observation year 1999/2000 of the Crab nebula.

3 Event reconstruction

The different arrival times of the signals from the individual heliostats were used to reconstruct the timing shower front of the individual events. The expected arrival times for all heliostats in each of the four cones were calculated and stored in a “library” for a 5×5 degree grid centered to a direction

about 1 degree offset from the current pointing direction of the heliostats. The offset was chosen to avoid a bias towards “correct pointing”. This calculation was performed assuming a point-like shower-maximum at a penetration depth of 230 g/cm^2 (the mean penetration of showers induced by a photon of 100 GeV) in the pointing direction. A spherical timing-front was assumed to be emitted by this maximum. The shower core was fixed at the geometrical centre of the field as defined by the used heliostats (it was verified that this assumption introduces no bias).

The measured arrival times were compared to the “library”. We define the time difference TIMEDIFF

$$\text{TIMEDIFF} = (\text{measured arrival time}) - (\text{nearest expected time from the library}) \quad (1)$$

The direction yielding the smallest χ_t^2 with

$$\chi_t^2 = \sum_i (\text{TIMEDIFF}_i)^2 \quad (2)$$

was chosen as the final reconstructed direction of the shower. Fig.2 shows projections of reconstructed directions in zenith and azimuth angle both for ON and OFF source directions for a large data sample. The origin corresponds to the pointing direction determined by the heliostat tracking. The directions of events in the “smooth background” extending to large off-axis angles were found to be systematically misreconstructed. This effect was used in the later analysis to normalise ON and OFF rates.

If the “misreconstructed” directions are excluded, the angular resolution σ_{63} (the opening angle within which 63 % of all events are contained) is 0.7° .

4 Data reduction

From a total measuring time of 32 hours, only nights in which all four detector channels and the heliostats in the field were functioning normally according to the recorded monitor files were chosen for further analysis. Furthermore, only data taken in “good nights”, i.e., with no clouds, low humidity, no dust, remained after our cuts. These “meteorological cuts” are severe under the weather conditions at the PSA. In the data sample on Crab in February/March 2000 only 22 % of all data taken on the Crab pulsar passed all cuts.

The fundamental problem of all Cherenkov experiments - especially for those attempting to detect an excess due to gamma-rays in the total rate - is the fact that the night-sky background ON- resp. OFF-source differs in general. This can influence the counting rate and analysis efficiency in various ways. Whereas random events can be removed (see section 6), the change of the effective trigger threshold due to different noise levels in ON and OFF is a more serious problem. Here, it was solved by applying a variable offline threshold, calculated from the measured noise level in the related traces.

One can attempt to find an ON-source excess in the total

Table 1. Currents (mean of 4 Cones), single trigger rate of charge integrating channel (mean of Cone 1+2), number of hardware-triggered events (“raw events”), decadic logarithm mean net-charge of all events in sample (“mean q”), number of events after angular reconstruction and software trigger (“rec. events”) and normalised number of events in central angular region (within 0.7 degrees of pointing direction) (“centr. events”) for the samples with pointing towards the Crab pulsar (“ON”) and on a sky position (“OFF”) with a right ascension 2.625 degrees smaller than in the ON direction. The total data-taking time ON was 430 minutes with an equal amount of OFF time.

	current [μA]	q-rate[kHz]	mean q	raw events	rec. events	centr. events
ON	19.0 ± 0.4	1.35	2.883 ± 0.004	68702	33384	9415
OFF	19.3 ± 0.3	1.49	2.876 ± 0.004	75198	33056	8678
EXCESS	-0.3	-0.14	0.007 ± 0.006	-6496	328 ± 258	737 ± 165

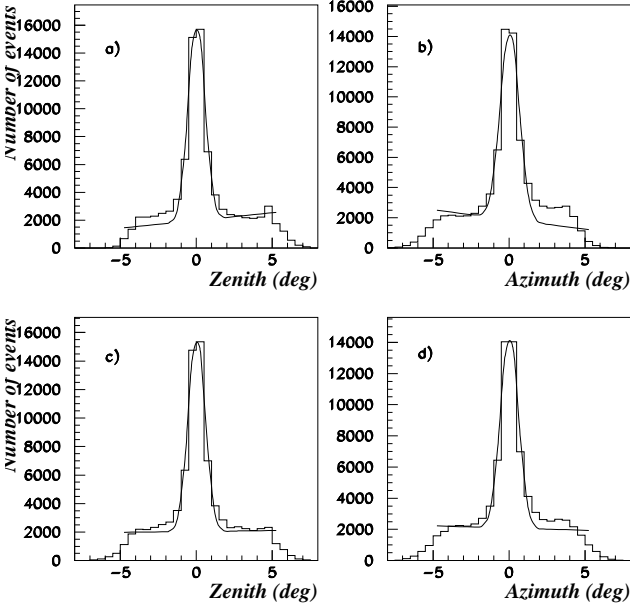


Fig. 2. Projections of the number of showers as a function of shower directions as reconstructed from the timing data. Shown is deviation of the reconstructed direction from the pointing direction on the elevation-axis (panels a. and c.) and azimuth-axis (panels b. and d.). The origin corresponds to the pointing direction as determined by the orientation of the heliostats. The data sample comprises of 32 hours of ON-source time on the Crab pulsar (panels a. and b.) and an equal amount of OFF-source time (panels c. and d.) taken under variable weather conditions in the season 1999/2000. The “Gaussian plus linear function” fit is performed to each subsample. It is seen that the Gaussian - corresponding to successfully direction reconstructed events - is always centred within $< 0.05^\circ$.

number of events (see section 6 below). A more sensitive method is to look for an excess in the central angular region. The normalised excess EXCESS_n was calculated according to the following equation:

$$\text{EXCESS}_n = \text{ON}_{\text{in}} - \text{OFF}_{\text{in}} \left(\frac{\text{ON}}{\text{OFF}} \right)_{\text{out}} \quad (3)$$

Here $(\text{ON}, \text{OFF})_{\text{in}}$ stands for the number of events within 0.7° from the source, resp. off-source direction, $(\text{ON}, \text{OFF})_{\text{out}}$ stands for the number of events with directions deviating more than 2° from the source direction.

5 Results

Several parameters of the data set taken on Crab pulsar are presented in table 1. Fig. 3 shows the number of events as function of angular distance from the source direction, both for ON- and OFF-source direction and the normalised difference ON-OFF. An excess of events in the angular region expected from Monte Carlo (MC) simulations (fig.3) is seen, we find $\text{EXCESS}_n = 737 \pm 165$ calculated according to eqn (3). The error is statistical. This corresponds to a 4.5σ excess and a mean excess rate $\text{EXCESS}_{\text{nr}} = 1.7/\text{min}$. An integral flux ϕ_{int} is calculated from this excess according to:

$$\phi_{\text{int}} = (\text{EXCESS}_{\text{nr}}/r_\gamma)(r_p/r_{\text{obs}})t_c\phi_{\text{whipple}} \quad (4)$$

Here $\phi_{\text{whipple}} = \int_{E_{\text{thresh}}}^{\infty} 3.3 \times 10^{-7} E^{-2.4} \text{m}^{-2} \text{s}^{-1} \text{TeV}^{-1} dE$ is the integral gamma-ray flux from the Crab above a threshold energy E_{thresh} as observed by the Whipple collaboration (A.M.Hillas et al. (1998)). r_γ is the gamma-ray rate expected in GRAAL from the MC simulated effective area for gammas based on this flux (0.011 Hz). Note that the absolute Whipple flux cancels in eq. (4), and we only adopt the spectral index from ref. (A.M.Hillas et al. (1998)). r_p is the proton rate expected in GRAAL on the basis of the known absolute differential flux of cosmic-ray protons ϕ_{ref} and the effective area for protons (4.0 Hz). r_{obs} is the observed cosmic-ray rate in the final reconstructed sample, corrected for dead time (1.6 Hz). The factor (r_{obs}/r_p) is an empirical correction for the fact that our MC calculated proton effective area predicts a somewhat higher proton rate than observed. t_c is a correction factor for the fact that some photons are expected in the “outer angular region” and was determined as 2.2 from MC data. The final integral flux above threshold assuming a differential spectral source index of -2.4 is:

$$\phi_{\text{int}} = 2.2 \pm 0.4 \text{ (stat)} \pm_{-1.5}^{+1.9} \text{ (syst)} \times 10^{-9} \text{ cm}^{-2} \text{ s}^{-1} \text{ above threshold}$$

6 Excess in total rate

If the detected excess (discussed in section 5) is real, one can estimate that there should be an excess of ≈ 2270 events within our measuring time. On the other hand, extrapolating the Whipple flux for Crab nebula (A.M.Hillas et al. (1998))

Table 2. Number of hardware-triggered events (“total events”), number of events once subtracted the accidental events and corrected for the dead time (“total corrected events”)

	Total events	Tot. correct. evs
ON	79194	58107
OFF	86428	58550
EXCESS	-7234 ± 575	-443 ± 483

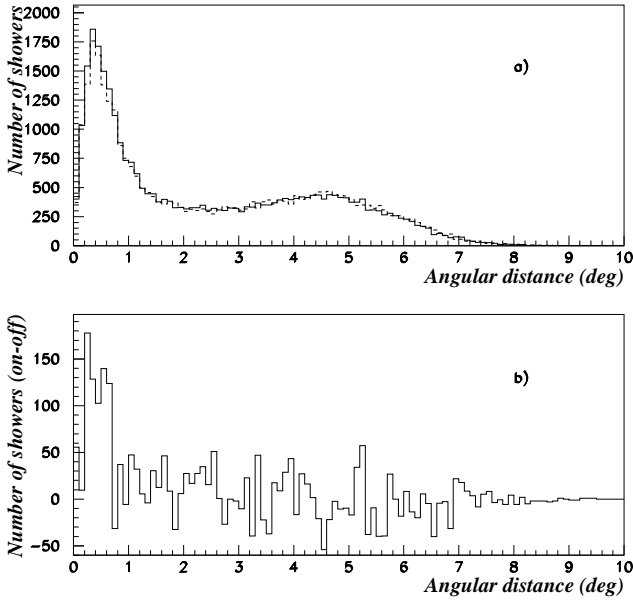


Fig. 3. The upper plot (a.) shows the number of events as a function of angular distance of reconstructed direction from source direction for ON-source events (full line) and OFF-source events (dashed line). No normalisation of any kind was applied to this plot. The lower plot (b.) shows the difference ON - OFF, normalised to the number of events in the outer angular region, according to eq. (3).

at our energy threshold, only 355 excess events are expected. With the hardware setting for the season 1999/2000 it could happen that the NSB triggers events (this was changed for the period 2000/2001). The rate of accidental events can be calculated from the single rates and subtracted from the total rate. Other corrections are related to the dead time of the setup. Table 2 right column shows the results of a careful correction for these effects for the data of the analyzed sample of Crab (see section 4). In the last column all the effects have been corrected and the total time of measurement is 430 min in ON position and the same time for OFF position. There is an excess in the OFF position of 7234 events in the hardware-triggered events. After subtraction of accidental events and corrections for dead time, the excess in the OFF position is only 443 events, which is within the statistical fluctuations. For orientation, a difference in the energy threshold of cosmic-ray protons between ON and OFF of

only 5GeV at an energy threshold of 2TeV already produces a difference of 550 events for the same time of measurement and using the known cosmic-ray proton flux and a constant effective area of 8000 m².

In an alternative approach the software analysis rejects accidental events due to the low number of peaks and uncorrelated times of the peaks of such events. Less than 0.6% of the accidental events pass the analysis for a very similar NSB to the one of Crab sample. In our analysis, a higher NSB rejects more accidental events. As seen in the column 5 of table 1 also here there is no significant excess in the total rate. This lack of an excess in the total rate seems to cast a doubt on the reality of the signal discussed in section 5.

7 Conclusion

The results of the present measurements do not prove that the use of an heliostat array in gamma-ray astronomy is a feasible alternative to the use of dedicated Cherenkov telescopes. The principle drawbacks of this approach were found to be the restricted field of view and the poor weather conditions at the relatively low elevation of the heliostat field not far from the sea (frequent high humidity at night). The field-of view restriction leads to a very similar time structure of the shower front in proton and gamma induced showers and biases the direction reconstruction based in timing towards to the pointing direction. Both effects together prevent any efficient separation of proton and gamma induced showers. This makes a flux determination independent of total rates difficult and severely limits the sensitivity of the experiment. The fraction of time (total duty cycle) with weather and moon-light conditions sufficient for the detection of gamma radiation was about 3-4 % at the PSA, about a factor of 5 lower than at astronomical sites. Both drawbacks seem to be unavoidable for the heliostat-field based approach also in the future.

Acknowledgements. The GRAAL project is supported by funds from the DFG, CICYT and the IHP “Access to large scale facilities” program of the EU. We thank the PSA - in particular A.Valverde - for excellent working conditions at the CESA-1 heliostat field.

References

- F.Krennrich, Proc. 7th Taipei Astrophysics Workshop, ASP Conference Series, Vol. XX, 2001, de. C.M. Ko, astro-ph/0101120.
- F.Arqueros, J.Ballestrín, M.Berenguel, D.M.Borque, E.F.Camacho, M.Díaz, R.Enríquez, H-J.Gebauer, R.Plaga, submitted to Astroparticle Physics.
- F.Arqueros, J.Ballestrín, D.M.Borque, M.Díaz, R.Enríquez, H-J.Gebauer, R.Plaga, these proceedings.
- M.C. Chantell et al. (STACEE coll.) astro-ph/9704037, Nucl.Inst.Meth. A408 (1998) 468.
- J.A.Zweerink et al., Proc. 26th ICRC 5 (1999) 223.
- M. de Naurois et al. (CELESTE coll.), astro-ph/0010265 (2000); J.Holder astro-ph/0010264 (2000).
- A.M.Hillas et al., Astrophys.J. 503 (1998) 744.